MEASURING WATER ICE CLOUD OPTICAL DEPTHS FROM MRO-CRISM MULTI-SPECTRAL IMAGES USING PCA/TT FOR SURFACE MODELING.

D. R. Klassen, *Rowan University, New Jersey, USA. (klassen@rowan.edu).*

Introduction

The water cycle on Mars plays an important role in its overall climate and "ground truth" measurements, over diurnal, seasonal, and inter-annual time scales, provide needed boundary conditions for models created to understand that climate. Throughout the years, it has become apparent that water ice clouds are an important aspect of the water cycle which is the motivation for this work.

There are two major difficulties to quantifying the water abundance in clouds. The first is that the radiative transfer modeling required to retrieve cloud optical depth is a function of the actual cloud particle sizes, shapes, their composition (amount of ice to dust nucleus) and the effect of dust aerosols on the spectral signature. There has been some work in this area (e.g. Ockert-Bell et al., 1997; Erard et al., 2000; Wolff et al., 2009) which has led to some usable constraints and approximations. The second is that one needs to know the surface spectral reflectance in order to model the atmosphere. Unfortunately, one needs to know how the atmosphere affects the measurements in order to retrieve the surface signature.

For this work, a synthetic surface model is created to address this issue. It uses both the actual collected data in concert with mineral spectral libraries to reconstruct "pure" spectral endmembers for the surface through two steps: principal components analysis (PCA) (Salmon, 1927) to find the underlying traits within the data based on their inherent variances, and target transformation (TT) (Bandfield et al., 2000) to recombine the principal components into the surface spectral endmembers. Each surface point can then be modeled as a linear combination of the endmembers. The coefficients for the endmembers, along with the optical depth for the dust and ice clouds, are the free parameters in a radiative transfer fit to the spectral data.

Data

This work uses near infrared (NIR) spectral images obtained by the Compact Reconnaissance Imaging Spectrometer for Mars (CRISM) in its multi-spectral mapping mode. In this mode, CRISM nominally collects 74-wavelength spectra using subsets from both of the two gratings (VNIR: 0.362–1.053 μm; IR: 1.002–3.920 μm) and builds up a map over several orbits in a sort of "raster-scan" technique. The frame rate of data collection is 15 or 30 Hz along track and spectra are binned 5:1 or 10:1 cross-track which gives a spatial resolution of 100 or 200 m. (Murchie et al., 2007).

These spectra were mapped into a rectangular array (i.e. cylindrically projected map) and averaged to a spatial resolution of $1/3^\circ \times 1/3^\circ$. In order to tie the spectra from the two detectors/gratings together, the VNIR 1.0233 μm measurements were averaged with the IR 1.0210 μm measurements and were assigned to wavelength 1.0222 μm. Additionally, the edge-of-detector wavelengths (0.3776, 1.0560, and 3.9435 μm) were removed due to the higher noise levels. Thus, for each sol we have a $1080 \times 540 \times 70$ (spatial map by wavelength) image data cube. Finally, to create a more complete map, data from about 20 mostly consecutive sols were combined into one image cube. In addition, another image cube of latitude by L_S by wavelength was created in order to more directly compare CRISM results with Mars Global Surveyor (MGS) Thermal Emission Spectrometer (TES) and Mars Odyssey (MO) Thermal Emission Imaging System (THEMIS) results (e.g. Smith et al., 2001a,b, 2003). The map of each sol was zonally averaged creating a latitude by wavelength array, then the arrays are stacked by the L_S for each sol. The particulars of the data are summarized in Table 1. The data Name is the year and day number of the central image in the set used to make the map and Color is the color used for that set in all graphs.

PCA Results

A complete discussion of the PCA process as applied to Martian spectral image cubes can be found in Klassen et al. (1999); a summary follows.

At its heart, PCA is a mathematical method of transforming an array from its original coordinate vector space, via translation and rotation, to a new vector space with basis vectors determined by the variance within the data itself. The new coordinate system is found by maximizing the variance/covariance of the data matrix which makes the basis vectors of the new space, eigenvectors, $\hat{e}_i$, of the data variance.

Dimensionality is reduced by retaining only the most significant eigenvectors/dimension. Significance is determined by the eigenvalues, which are a measure of how much of the data variance is described by that eigenvector; in all the data analyzed here over 80% of the total variance is accounted for in the first four eigenvectors. In many cases, the first four eigenvectors can account for over 99% of the total variance and in most cases, it is over 95%. This means that the data only have at most

Table 1: CRISM Data Summary

Name	Nominal Date	Start Date – End Date	# of Days	Median L_S	Color
2006_321	17 NOV 2006	08 NOV 2006 – 25 NOV 2006	18	136.7°	Red
2007_071	12 MAR 2007	01 MAR 2007 – 30 MAR 2007	22	198.8°	Green
2007_170	19 JUN 2007	04 JUN 2007 – 03 JUL 2007	30	260.6°	Blue
2007_261	18 SEP 2007	08 SEP 2007 – 28 SEP 2007	21	316.0°	Brown
2008_012	12 JAN 2008	28 DEC 2007 – 27 JAN 2008	31	016.4°	Cyan
2008_167	15 JUN 2008	31 MAY 2008 – 25 JUN 2008	21	085.6°	Orange
all L_S map	image of latitude v. L_S with each day meridianally averaged				Gold

five inherent dimensions that describe almost all the data variance.

In previous work (Klassen and Smith, 2010) it was found that due to the nature of the $\hat{e}_0$ and its tie to "brightness", the residual polar cap regions and the visible wavelengths regime creates significant confusion in the eigenvectors. For this reason, these geographical and spectra regions were removed from the analysis. Additionally, the 2 μm band, which is due mostly to atmospheric CO_2 was also removed from the analysis.

The resulting PCA eigenvector spectra for all seven data sets are plotted in Figure 1. As typical in PCA, each eigenvector represents some general trait—the meaning of which we can glean from the spectral shape as well as the geographic regions that have the largest (or smallest) contribution to it. For these data $\hat{e}_0$ represents overall Mars NIR brightness—it is greatest in the standard bright albedo regions and least in the standard dark albedo regions. For $\hat{e}_1$, it is greatest in regions that are cold and covered by ice clouds and fogs or surface frosts in subpolar regions. The last two significant eigenvectors tend to follow geographic regions so are interpreted as representative of surface variation. Additionally, we can see great similarity in $\hat{e}_0$. There is some level of broad similarities across all dates in the the other three eigenvectors, but less so. In general, the eigenvectors for the L_S-map data look like a sort of median spectrum of all the other six. The goal will be to use these eigenvectors as a universal set in order to create a universal set of spectral endmembers.

TT Results

The technique of target transformation is a way to recover spectral endmembers for a data set without making any a priori choices from within the set itself. The idea is that, through PCA we have found the underlying traits in the data that lead to the greatest variation, then we recombine those eigenvectors in an attempt to recover the spectral endmembers that led to these eigenvectors being the source of underlying variance. To find those endmember linear combinations we compare them to a large spectral library—the process creates the best fit linear combination to each of these "target" spectra. The resulting transformed eigenvectors are our candidate endmembers. When plotted in PC-space, the candidates form a data cloud. The results of using individual date PCs in the the TT process are presented in Figure 2. At this point, only 2006_321 and 2008_167 have been run in this way as individual tests (Klassen, 2012).

As there were four significant PCA dimensions, the endmember cloud in PC-space should be bounded by five vertices; these five points are taken as the spectral endmembers of the data. In order to test the technique, only two of the five were chosen to be spectral endmembers for the radiative transfer model. Along with the parameters τ_{dust}, τ_{ice}, the surface reflectance is created by linearly combining the endmembers, such that $A = \sum \alpha_i E_i$ where the Es are the endmember spectrum and αs are the mixing coefficients—these coefficients are free parameters in the fitting model.

Radiative Transfer Results

Due to the vast amount of data points, attempting to perform a χ^2-minimization fit to each spectrum in order to recover the four parameters, a look-up table of radiative transfer models was created using the technique of Wolff et al. (2011). Each of the four parameters was varied over a selected range and a radiative transfer model created for each combination. This resulted in a table, for each date, of over 203000 model spectra. Each data point is then compared to all the pre-created models and the best fitting one, in a χ^2 sense, is chosen.

I will present the resulting maps of ice and dust optical depths. In addition I will report on the status of the creation of "universal" endmembers to be used in the creation of a "universal" look-up table of radiative transfer models.

Acknowledgements

CRISM data were preprocessed into forms usable by this project by Michael D. Smith of Goddard Space Flight Center. Radiative transfer code-base provided by Michael Wolff of Space Science Institute.

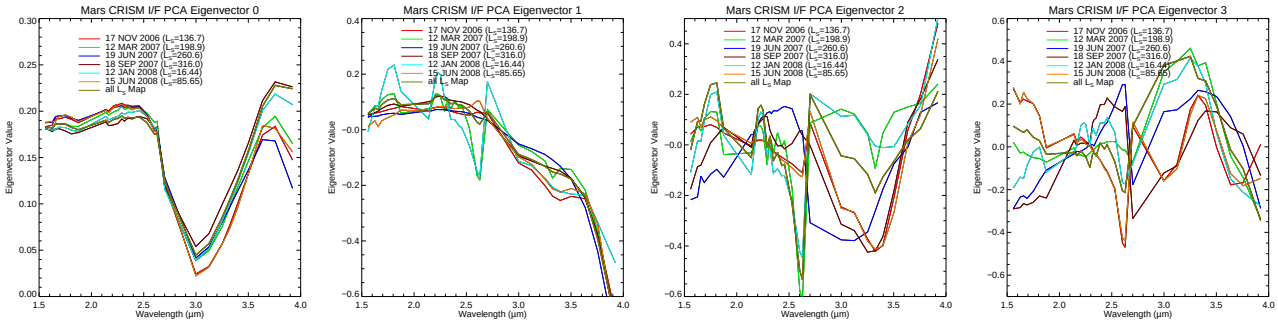

(a) $\hat{e}_0$— "brightness" (b) $\hat{e}_1$— "iciness" (c) $\hat{e}_2$— "primary geology" (d) $\hat{e}_3$— "local geology"

Figure 1: CRISM eigenvector spectra.

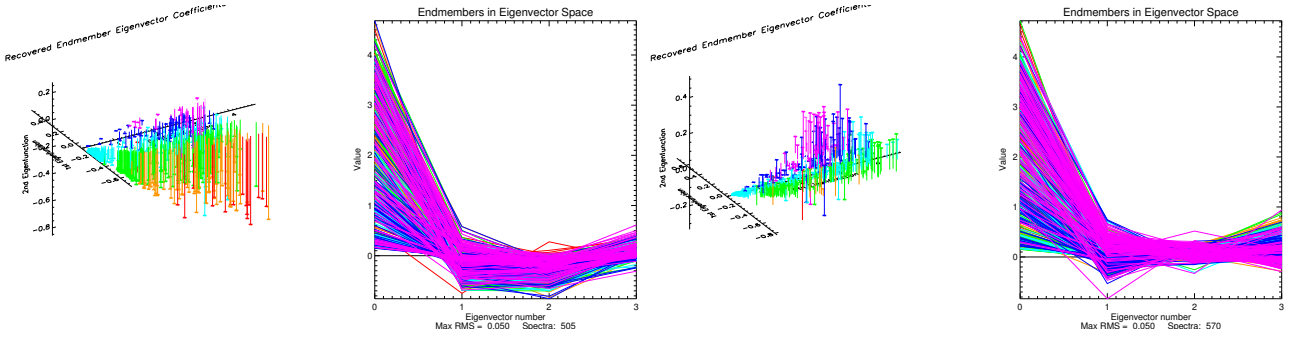

(a) 2006_321 PC scatter plot (b) 2006_321 PC spectra (c) 2008_167 PC scatter plot (d) 2008_167 PC spectra

Figure 2: CRISM candidate endmembers for 2006_321 and 2008_167. The endmember candidates are plotted as PC-spectra in (a) and (c) and as points in PC-space in (b) and (d). Colors for the spectra are only cosmetic—to help see the multitude of spectra. Colors for the scatter plots are indicative of the value in the vertical dimension in order to better visualize the 3-D plot.

This work has been supported by NASA Mars Data Analysis Program (NAG5-11076) and by both the National Science Foundation Planetary Astronomy and Research at Undergraduate Institutions programs (0307924 and 1008744).

References

Bandfield, J. L., Christensen, P. R., Smith, M. D., Apr. 2000. Spectral data set factor analysis and end-member recovery: Application to analysis of Martian atmospheric particulates. J. Geophys. Res. 105, 9573–9588.

Erard, S., Lellouch, E., Encrenaz, T., Morris, P., de Graauw, T., Burgdorf, M., Mar. 2000. Composition of Martian Surface Materials and Dust from ISO Observations. In: Lunar and Planetary Institute Conference Abstracts. Vol. 31. p. 1325.

Klassen, D. R., Oct. 2012. Surface Spectral Endmember Recovery of CRISM Mapping Data for Radiative Transfer Modeling. In: AAS/Division for Planetary Sciences Meeting Abstracts. Vol. 44. p. 214.20.

Klassen, D. R., Bell, J. F., Howell, R. R., Johnson, P. E., Golisch, W., Kaminski, C. D., Griep, D., Mar. 1999. Infrared Spectral Imaging of Martian Clouds and Ices. Icarus 138, 36–48.

Klassen, D. R., Smith, M. D., Oct. 2010. Preliminary PCA/TT Results on MRO CRISM Multispectral Images. Bulletin of the American Astronomical Society 42, 1027.

Murchie, S., Arvidson, R., Bedini, P., Beisser, K., Bibring, J.-P., Bishop, J., Boldt, J., Cavender, P., Choo, T., Clancy, R. T., Darlington, E. H., Des Marais, D., Espiritu, R., Fort, D., Green, R., Guinness, E., Hayes, J., Hash, C., Heffernan, K., Hemmler, J., Heyler, G., Humm, D., Hutcheson, J., Izenberg, N., Lee, R., Lees, J., Lohr, D., Malaret, E., Martin, T., McGovern, J. A., McGuire, P., Morris, R., Mustard, J., Pelkey, S., Rhodes, E., Robinson, M., Roush, T., Schaefer, E., Seagrave, G., Seelos, F., Silverglate, P., Slavney, S., Smith, M., Shyong, W.-J., Strohbehn, K., Taylor, H., Thompson, P., Tossman, B., Wirzburger, M., Wolff, M., May 2007. Compact Reconnaissance Imaging Spectrometer for Mars (CRISM) on Mars Reconnaissance Orbiter (MRO). Journal of Geophysical Research (Planets) 112 (E11), 5.

Ockert-Bell, M. E., Bell, J. F., Pollack, J. B., McKay, C. P., Forget, F. ., Apr. 1997. Absorption and scattering properties of the Martian dust in the solar wavelengths. J. Geophys. Res. 102, 9039–9050.

Salmon, G., 1927. A Treatise on the Analytic Geometry of Three Dimensions. Chelsea Publishing Company, New York.

Smith, M. D., Bandfield, J. L., Christensen, P. R., Richardson, M. I., Nov. 2003. Thermal Emission Imaging System (THEMIS) infrared observations of atmospheric dust and water ice cloud optical depth. J. Geophys. Res. (Planets) 108, 1–1.

Smith, M. D., Pearl, J. C., Conrath, B. J., Christensen, P. R., Nov. 2001a. One Martian year of atmospheric observations by the Thermal Emission Spectrometer. Geophys. Res. Lett.28, 4263–4266.

Smith, M. D., Pearl, J. C., Conrath, B. J., Christensen, P. R., Oct. 2001b. Thermal Emission Spectrometer results: Mars atmospheric thermal structure and aerosol distribution. J. Geophys. Res. 106, 23929–23945.

Wolff, M. J., Clancy, R. T., Cantor, B., Madeleine, J.-B., Feb. 2011. Mapping Water Ice Clouds (and Ozone) with MRO/MARCI. In: Forget, F., Millour, E. (Eds.), Mars Atmosphere: Modelling and observation. pp. 213–216.

Wolff, M. J., Smith, M. D., Clancy, R. T., Arvidson, R., Kahre, M., Seelos, F., Murchie, S., Savijärvi, H., Jun. 2009. Wavelength dependence of dust aerosol single scattering albedo as observed by the Compact Reconnaissance Imaging Spectrometer. Journal of Geophysical Research (Planets) 114 (E13), 0–+.